

Structure-based design of the first potent and selective inhibitor of human non-pancreatic secretory phospholipase A₂

R.W. Schevitz, N.J. Bach, D.G. Carlson, N.Y. Chirgadze, D.K. Clawson, R.D. Dillard, S.E. Draheim, L.W. Hartley, N.D. Jones¹, E.D. Mihelich, J.L. Olkowski, D.W. Snyder, C. Sommers², and J.-P. Wery

A lead compound obtained from a high volume human non-pancreatic secretory phospholipase A₂ (hnps-PLA₂) screen has been developed into a potent inhibitor using detailed structural knowledge of inhibitor binding to the enzyme active site. Four crystal structures of hnps-PLA₂ complexed with a series of increasingly potent indole inhibitors were determined and used as the structural basis for both understanding this binding and providing valuable insights for further development. The application of structure-based drug design has made possible improvements in the binding of this screening lead to the enzyme by nearly three orders of magnitude. Furthermore, the optimized structure (LY311727) displayed 1,500-fold selectivity when assayed against porcine pancreatic s-PLA₂.

Lilly Research Laboratories, Lilly Corporate Center, Eli Lilly and Company, Indianapolis, Indiana 46285, USA

¹Present address: Molecular Structure Corp., The Woodlands, Texas 77381, USA

²Present address: Washington University School of Medicine, St. Louis, Missouri 63110, USA

Correspondence should be addressed to R.W.S.

Exceptionally high levels of hnps-PLA₂ have been found in synovial fluid from inflamed joints of arthritic patients as well as in the blood of patients with acute pancreatitis, adult respiratory distress syndrome (ARDS), bacterial peritonitis and septic shock¹. This protein is a 14,000 M_r, Ca²⁺ dependent enzyme which indiscriminately hydrolyzes phospholipids at the *sn*-2 position, yielding free fatty acid and lysophospholipid². Lipid mediators of inflammation that may result from this catalytic activity include all eicosanoids and platelet activating factor as well as various lysophospholipids that are lytic to cells³. Since the disease states delineated above are characterized by inflammation that is out of control, it has been hypothesized that hnps-PLA₂ may be a key contributor to the morbidity and mortality experienced by these patients⁴. While this concept has been challenged⁵, there is general agreement that only the clinical evaluation of a potent and selective inhibitor of this enzyme will unravel its role in these various and deadly disorders⁶.

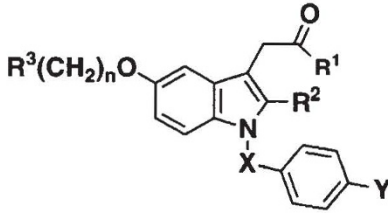
Structural information has been successfully used for drug design and development in several target proteins. These include inhibitors for carbonic anhydrase⁷ (glaucoma), thymidylate synthase⁸ (cancer), HIV protease^{9,10}, (AIDS), purine nucleoside phosphorylase¹¹ (T-cell mediated diseases)¹², sialidase (influenza) and elastase¹³ (emphysema). Previous attempts to design PLA₂ inhibitors have utilized the structurally related, but non-identical snake venom and pancreatic enzymes for inhibitor optimization. Consequently, while some of these compounds have shown weak inhibition of hnps-PLA₂^{14,16}, they are usually as potent or more potent inhibitors of

pancreatic s-PLA₂. To meet our goal of selective inhibition of hnps-PLA₂, we chose to screen exclusively against this enzyme. Large scale preparation of recombinant enzyme enabled us to meet these screening goals¹⁷ and was crucial to the successful implementation of a structure-based drug design strategy.

The structure of native hnps-PLA₂ has been determined in two crystal forms^{17,18}. The structure of a complex of the human enzyme with a phosphonate transition state analogue¹⁸ (TSA) has also been determined. This inhibitor shows the same mode of binding as is seen with the snake¹⁹ and bee venom enzymes²⁰. The structure of a mutant porcine enzyme with an amide substrate analogue²¹ (ASA) shows many similarities to TSA binding. Together these substrate analogues provide valuable information for identifying and characterizing the functional groups in the enzyme active site which are important for interacting with substrate. These are also key interactions which might be exploited in the development of inhibitors for pharmaceutical purposes.

Initial screening lead

The lead compound, indole 1 (Table 1), was found during large scale screening using an *Escherichia coli* membrane assay. 1 is structurally related to the well-known anti-inflammatory drug, indomethacin (2), which is a potent cyclooxygenase inhibitor and has been reported to weakly inhibit rabbit²² and human²³ s-PLA₂ enzymes. Indole 1 was later tested with a newer chromogenic screening assay using a thiol substrate analogue²⁴ and gave an IC₅₀ (concentration required for 50 % enzyme inhibition) of 0.014 mole fraction. In addition, selected

Table 1 Structure-activity relationship for substituted indoles


Indole	R¹	R²	R³	n	X	Y	X _{1/2} (50)	Tissue-Based Assays		
								hnps-PLA ₂ App.K _B	AA Selectivity	
Indomethacin	1	OH	CH ₃	H	1	CH ₂	H	.014	2.89	15.8
	2	OH	CH ₃	H	1	C=O	Cl	.058	0.03	0.98
	3	NH ₂	CH ₃	H	1	CH ₂	H	.00068	3.43	44.8
	4	NH ₂	CH ₃	CO ₂ H	1	CH ₂	H	.0018	8.22	NE
	5	NH ₂	CH ₃	CO ₂ H	2	CH ₂	H	.00035	3.76	NE
	6	NH ₂	CH ₃	CO ₂ H	3	CH ₂	H	.00012	2.38	NE
	7	NH ₂	CH ₃	CO ₂ H	4	CH ₂	H	.00075	8.8	NE
	8	NH ₂	CH ₃	PO ₃ H ₂	3	CH ₂	H	.000045	0.85	NE
	9	NH ₂	H	PO ₃ H ₂	3	CH ₂	H	.00016		
LY311727	10	NH₂	CH₂CH₃	PO₃H₂	3	CH₂	H	.000019	0.27	NE
LY314024	11	NH₂	(CH₂)₂CH₃	PO₃H₂	3	CH₂	H	.005	6.2	
	12	NH₂	CH₂CH₃	PO₃H₂	3	CH₂	Ph	.0025		

The mole fractions for 50 % inhibition $X_{1/2}(50)$ were calculated using the chromogenic assay. In the tissue-based assay the calculated apparent K_B represents the concentration of drug (μM) which doubles the concentration of agonist to achieve an equivalent response. AA selectivity represents the concentration of drug (μM) which doubles the control ED_{50} (concentration of agonist required to elicit 50 % of the maximal response) value which may not be determined at equivalent responses. NE = no effect, which represents no rightward shift or suppression of the drug-treated curves relative to the control curves at 10–30 μM of drug.

inhibition) of 0.014 mole fraction. In addition, selected indoles were evaluated in a secondary tissue-based assay (TBA) where guinea pig lung pleural strips served as 'natural substrate' for hnps-PLA₂. The tissues were challenged with hnps-PLA₂ (ref. 25) resulting in the catalytic release of arachidonic acid and the subsequent formation of primarily cyclooxygenase (CO) products leading to the measured contractile responses. Because this TBA measures the catalytic activity of hnps-PLA₂ indirectly, the potency of some agents that act down stream to PLA₂ (that is CO inhibitors) will be over estimated (see indomethacin Table 1). To eliminate this problem, the tissues were challenged in the presence or absence of drug with exogenously administered arachidonic acid (AA) which circumvents the PLA₂ step. Any agent like indomethacin that demonstrates suppression of the AA responses can be ruled out as a specific inhibitor of PLA₂. Thus appropriate control experiments are critical to characterizing novel and specific inhibitors of hnps-PLA₂ in this assay. An apparent K_B (Table 1) of 2.89 μM was determined for indole 1 in the TBA. The activity of indole 1 in the TBA resulted from its combined inhibition of hnps-PLA₂ and CO. Nonetheless, the combination of results from isolated enzyme and tissue bath experiments encouraged us to pursue a structure-based drug design approach to the optimization of this mol-

ecule and elimination of the CO component.

In order to visualize this interaction, crystals of the complex between indole 1 and hnps-PLA₂ were grown. These were hexagonal and diffracted to 2.7 Å resolution (Table 2). The inhibitor is located at the active site in the previously described hydrophobic channel¹⁷ (Figs 1a, 2). The cavity changes structure in two significant ways to accommodate the inhibitor (Fig. 2). Firstly, the narrow region in the native structure bounded by residues 20–24 on one side of the channel and His 6 on the opposite side enlarges by the displacement of the His 6 side chain away from the pocket and into a more solvent exposed position. The benzyl group of indole 1 then fits into this vacated space lining the main cavity. This is similar to the movement seen in His 6 on binding of the TSA to hnps-PLA₂ (ref. 18) and in Arg 6 on binding ASA to porcine PLA₂ (ref. 21). Secondly, the flap residue Lys 69 and Leu 2 at the base of the amino-terminal helix move away from each other to accommodate the 5-O-methyl group of 1, which points away from the calcium binding loop and fits into the space created between these two residues. No counterpart to this movement is seen with either of the substrate analogues^{18,21}.

The 3-acetate group of 1 is located deep in the cavity and interacts directly with Asp 49 (Figs 1a, 4a). The two side chain oxygens of Asp 49 normally provide two of

Table 2 Summary of the crystallographic data for the four complexes whose structure have been solved

indole	1	3	6	8
space group	P6 ₁ 22	P6 ₁ 22	P6 ₁ 22	P6 ₁ 22
cell parameters:				
a Å	76.4	76.2	76.4	77.0
c Å	89.4	91.5	91.6	91.6
Resolution Å	2.7	2.2	2.2	1.8
Completeness %	72	78	70	76
R _{merge} % ¹	8.3	9.2	9.0	6.3
r.m.s.d. from target values:				
bond lengths Å	0.012	0.017	0.018	0.019
bond angles (°)	1.9	1.8	2.1	2.0
number of waters	0	40	95	102
R-factor (%) ²	20.9	19.6	17.2	18.4

¹ $R_{\text{merge}} = \sum |I_i - \langle I_i \rangle| / \sum I_i$, where I_i is the intensity of an individual measurement, and $\langle I_i \rangle$ is the mean intensity of this reflection

² $R\text{-factor} = \sum ||F_o| - |F_c|| / \sum |F_o|$, where $|F_o|$ and $|F_c|$ are the observed and calculated structure factors respectively.

site calcium is seen in this structure, despite crystallization conditions using ample calcium (10mM) and clear presence of a 'second' calcium site near the main chain carbonyls of Phe 24, Gly 26 and Tyr 120¹⁸. Instead, the Asp 49 side chain moves 1 Å from the native position toward the acetate group of **1**, with one Asp 49 side chain oxygen 2.5 and 2.7 Å respectively from the acetate oxygens of **1**. Apparently this Asp 49 side chain oxygen is protonated and forms a bifurcated hydrogen bond to both acetate oxygens of the inhibitor (Figs 1a, 3c, 4a). Neither acetate oxygen of indole **1** is in a good position to hydrogen bond to the active site His 48, which has rotated about 50° from its position in the native structure. The displacement of the active site calcium by the acetate of **1** is consistent with other observations that this

calcium is weakly bound with an apparent K_m of 1.5 mM (ref. 24). This accommodation of indole **1** occurs without any concerted movement of main chain atoms in the enzyme.

Comparison with enzyme/substrate interactions

It was useful to compare the binding of indole **1** to hnp-PLA₂ with the binding of TSA to hnp-PLA₂ and ASA to porcine PLA₂. This was done by positioning the substrate analogues in the hnp-PLA₂ cavity by superpositioning the α -carbon positions of their respective PLA₂s on the corresponding positions of hnp-PLA₂ (not shown). Despite some key differences between the two substrate analogues and the use of different PLA₂s, homologous atoms are located very close to each other, with near identity between equivalent *sn*-1 and *sn*-3 substituent atoms. The long *sn*-2 chains of both analogues occupy slightly displaced parallel positions that fit nicely into the space taken in their native structures by their respective side chains of residue 6. Some similarities are seen in comparing the binding of TSA and ASA to PLA₂ with that of indole **1** to hnp-PLA₂, despite entirely different underlying structures (Fig. 3a–c). The indole ring of **1** approximates the positions of the glycerol backbone of TSA and the first few substituent atoms on *sn*-1 and *sn*-2. Also, the *N*-benzyl group of **1** follows the natural bend of the *sn*-2 chain into the slot formed in the side of the amino-terminal helix at His 6. With its multiple ring structure, indole **1** is a more conformationally constrained molecule than either substrate analogue. It fortuitously has the necessary shape to fit into the same cavity and possesses potency approaching that of TSA ($IC_{50} = 0.0032$ mole fraction).

Both TSA and ASA make several similar polar interactions with PLA₂. Note first that each contributes a ligand to the active site calcium in the form of an oxygen atom that is closely linked to the *sn*-2 position. This ligand is a non-bridging oxygen of the phosphonate in TSA (Fig. 3a) and the amide carbonyl in ASA (Fig. 3b). In contrast, the indole **1** complex with hnp-PLA₂ completely lacks this active site calcium. While either oxygen from the 3-acetate group could plausibly be such a ligand because of its close proximity to the usual calcium site, both instead interact directly with Asp 49. The analogues also form hydrogen bonds to the active-site His 48 (ref. 26). TSA can hydrogen bond through the other non-bridging phosphonate oxygen (Fig. 3a) when His 48 is

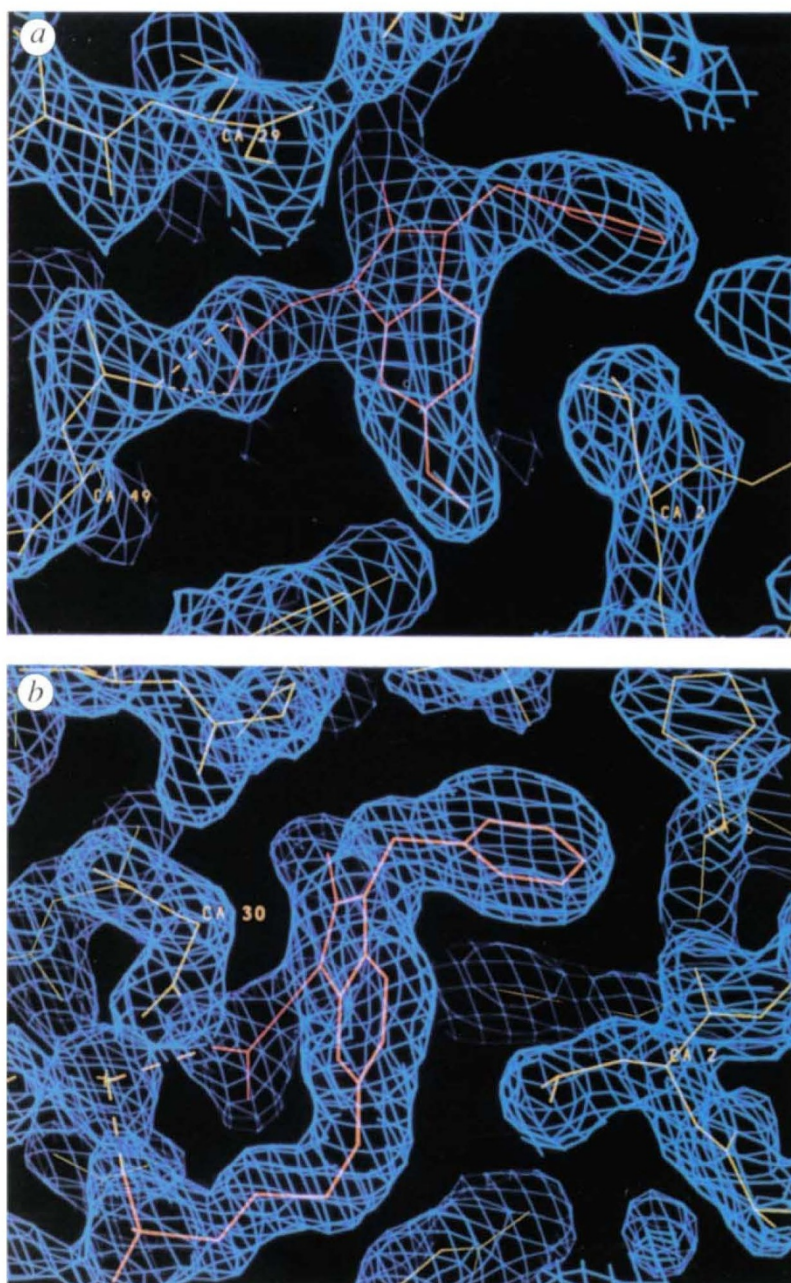


Fig. 1 a, 2.7 Å resolution electron density map (blue) and skeletal structure (yellow) of hnp-PLA₂ in the region of the active site cavity showing binding of the lead compound indole **1** (red). The map is contoured at 1.0 σ , with coefficients $2F_o - F_c$ and phases determined and refined as summarized in Table 2. The structure of **1** shows the direct hydrogen-bonding (dashed lines) to Asp 49 and absence of the active site calcium normally linked to Asp 49. b, 1.8 Å resolution electron density map (blue) and skeletal structure of hnp-PLA₂ (yellow) as in (a) showing binding of indole **3** (red). Amide oxygen and phosphonate oxygen provide two of the seven ligands (dashed lines) to calcium (cross).

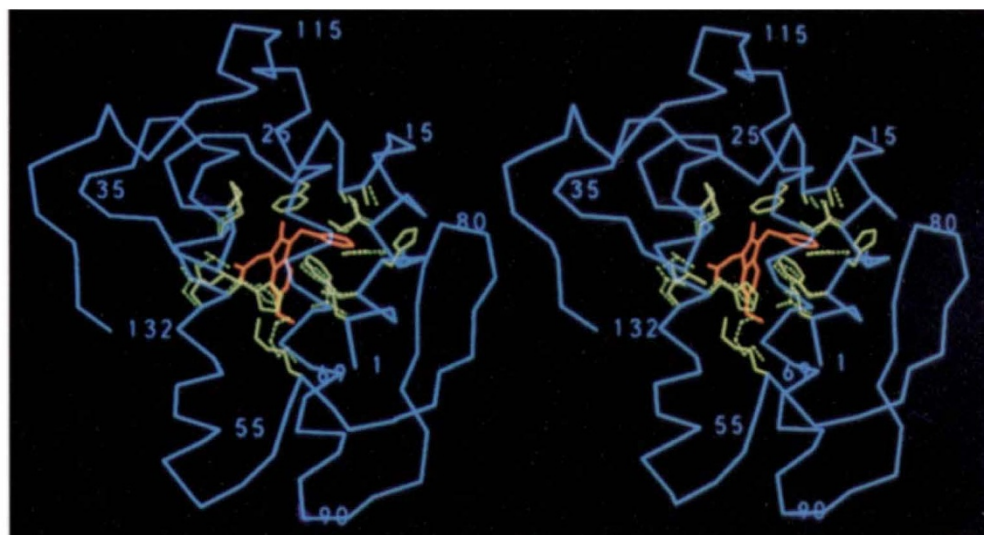


Fig. 2 Relative binding of indole **1** (red) in $C\alpha$ model of hnpS-PLA₂ (blue). Side chains of residues lining the cavity are shown (green) for both native (dashed) and inhibitor bound (solid) structures. Note the movement of the His 6 side chain, which partially overlaps the benzyl group of the inhibitor in the native structure, away from the binding pocket and into a more solvent exposed position in the complex.

protonated at lower pH, and ASA can hydrogen bond through its amide nitrogen (Fig. 3b) when His 48 is not protonated at higher pH.

Progression to indole 8

As a first step in improving indole **1** we sought to mimic the interactions of the substrate analogues at the active site both by providing an oxygen ligand to the active site calcium (rather than displacing it) and by forming a hydrogen bond to His 48. The structure of the ASA complex shows that an amide at this position can fulfill both functions (Fig. 3b). This suggested that the replacement of the 3-acetate group of indole **1**, which is in approximately the equivalent position as the amide of ASA, with an acetamide might mimic the desired interactions. That replacement yielded indole **3** (Table 1), which has a 20-fold enhanced activity in the chromogenic assay. The lack of a corresponding increased potency in the TBA is probably related to the anomalously low apparent K_b for indole **1** which results from the combined inhibition of both hnpS-PLA₂ and CO and thus masks the improvement of **3**. The threefold decrease in activity of indole **3** toward the arachidonic acid responses indicates less inhibition of CO and a closer approximation of its true potency toward hnpS-PLA₂ in this assay. The crystal structure of this complex was determined (Table 2) and shows that the desired features were obtained. The active site calcium is retained (Fig. 4b) with the amide oxygen providing one of the calcium ligands. Like ASA, the amide nitrogen hydrogen bonds to His 48, however, there is a significant adjustment in the orientation of the indole ring when compared with **1**. The end of the ring containing the 5-O-methyl group swings 1.5 Å closer to the calcium binding loop, and the methyl group reverses its orientation in the cavity by swinging away from the base of the N-terminal helix and pointing toward the calcium binding loop. This is a movement of the methyl group of over 5 Å. The Lys 69 side chain slides toward

the N-terminal helix to close up the space created by this movement of inhibitor. The N-benzyl group adjusts slightly to the movement of the attached indole and remains bound in essentially the same way in its pocket off the main cavity.

A further comparison of the binding of indole **3** (and **1**) with that of TSA and ASA shows that another important polar interaction with the active site calcium, which takes place through the *sn*-3 phosphate of both TSA and ASA, is missing in these indoles (Fig. 3a-d). In each of the substrate analogues, one non-bridging oxygen of the phosphate provides a ligand for the calcium, and the other non-bridging oxygen forms a hydrogen bond to the side chain of residue 69 (either a lysine or tyrosine). In contrast indole **3** does not even extend into this region. But a convenient means by which to mimic the phosphate interactions of TSA and ASA is suggested by the orientation of the 5-O-methyl group of **3**. It now points towards the calcium binding loop and fortuitously also points towards the interaction sites occupied by the phosphates of the substrate analogues. Thus modification at this 5 position offers the opportunity to emulate the phosphate of the substrate analogues. A carboxylate was selected as a synthetically convenient group that could be linked here to provide an additional oxygen ligand for the calcium and also hydrogen bond to Lys 69. Indoles **4**, **5**, **6** and **7** with spacers of one, two, three and four methylenes respectively (Table 1) were synthesized and tested for activity. Indoles **5** and **6** both showed improved activity compared to **3** with the highest activity occurring with the three carbon linkage of **6**. The activity of indole **6** improved more than fivefold over that of **3**. Indole **4**, with the short one carbon spacer, actually shows loss in activity compared to **3**. Indole **6** was the most potent among these four compounds in the TBA. It is significant that the CO component in the TBA was also eliminated so that all of the observed activity of indole **6** is directed toward inhibition of hnpS-PLA₂.

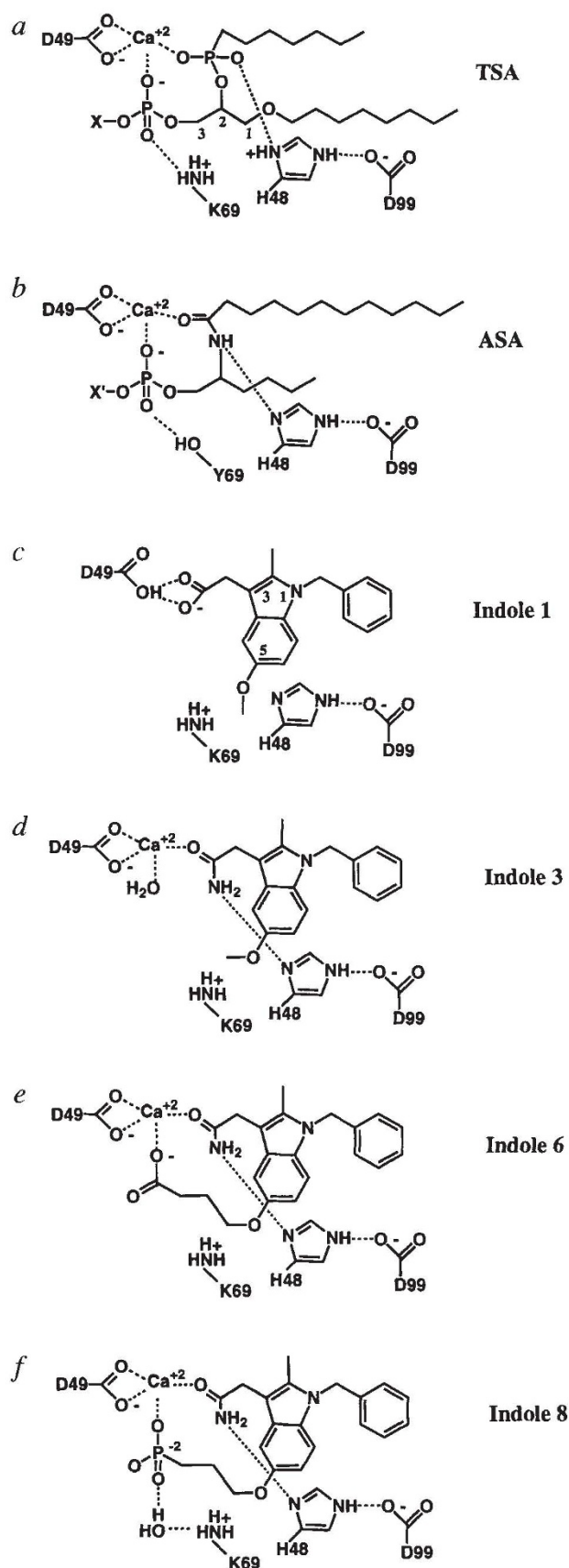


Fig. 3 Schematic representation of inhibitor binding to PLA_2 . *a*, binding of TSA to hnpS- PLA_2 shows three important interactions to the enzyme: a hydrogen bond to a protonated His 48 and two oxygen ligands to the active site calcium from the *sn*-2 phosphonate and *sn*-3 phosphate. *b*, binding of ASA to porcine PLA_2 also shows three strong interactions: a hydrogen bond from the amide nitrogen to an unprotonated His 48 and two oxygen ligands to the calcium from the amide carbonyl and the *sn*-3 phosphate. *c*, Binding of the lead compound indole **1** to hnpS- PLA_2 makes a bifurcated hydrogen bond to Asp 49, displacing the calcium. There is no interaction with His 48. *d*, binding of indole **3** to hnpS- PLA_2 with an amide that hydrogen bonds to His 48 and provides an oxygen ligand to the calcium. *e*, binding of indole **6** to hnpS- PLA_2 adds a carboxylate extending from the 5-position to provide a second calcium ligand from inhibitor. *f*, binding of indole **8** to hnpS- PLA_2 uses a phosphonate extending from the 5-position to provide the second calcium ligand.

The crystal structure of indole **6** bound to hnpS- PLA_2 was also determined (Table 2). The structure revealed that **6** binds in a manner very similar to **3**, with the indole ring, the benzyl substituent and the amide group all in essentially identical positions (Fig. 4c). The 5-carboxy substituent reaches out between Lys 69 and the active site calcium to provide a ligand for the calcium, as planned (Fig. 3e). The intended hydrogen bond to Lys 69 is not formed since the trigonal carboxylate points away from Lys 69.

In order to better emulate the phosphate interactions of TSA and ASA with both the active site calcium and residue 69 and perhaps achieve better binding, indole **8** was synthesized. It has a phosphonate, which is a close analogue of phosphate, on the 5 position instead of a carboxylate (Fig. 3f). This resulted in a nearly threefold increase both in binding to the enzyme and activity in the TBA (Table 1). The crystal structure of the complex with **8** was also determined (Table 2) and confirms that the phosphonate provides an oxygen ligand to the active site calcium (Figs 1b, 4d). A hydrogen bond to Lys 69 is also present, although it is mediated by a water molecule. Thus the tetrahedral geometry of the phosphonate allows one oxygen to point toward Lys 69 whereas the carboxyl of indole **6** cannot. However, the 5 Å distance from this oxygen of the phosphonate group to Lys 69 in indole **8** places it too far from Lys 69 to hydrogen bond directly. Efforts to further optimize this interaction are continuing.

Studies leading to LY311727

There is good correlation between the crystal structures and the activity of inhibitors substituted at various positions on these indoles. There is limited room, for instance, between the 2-methyl group and the cavity wall. Our binding studies show that having a slightly larger group at this position actually improves binding presumably by making better hydrophobic contact with the short helix (residues 16–24) forming the cavity wall here. Thus, LY311727 (**10**) with an ethyl group at R^2 is about threefold more potent in both assays than indole **8** with a methyl (Table 1), but the slightly larger propyl group at R^2 (indole **11**) kills activity with over 250-fold loss in

binding compared with LY311727. This is also consistent with a marked decrease in activity of 11 in the TBA. In contrast, indole 9 with just a hydrogen at R² has a

fivefold lower potency than indole 8. Modifications at Y (Table 1) on the benzyl ring have the expected effect; the structure shows that this *para* position is buried in the side of the N-terminal helix and points directly into the main chain atoms. This is consistent with observations that indole 12 with a phenyl at Y has over 100-fold lower activity than LY311727. Similarly the fourfold lower activity of indomethacin (indole 2) compared with indole 1 probably arises in part from its chloro substitution at Y. In the TBA LY311727 (at 0.1–10 μM) suppressed the contractile responses induced by hnpS-PLA₂ in a concentration related manner (Fig. 5a). The apparent dissociation constant (K_B) was calculated at $0.27 \pm 0.05 \mu\text{M}$. The activity of LY311727 against hnpS-PLA₂ is in sharp contrast to its effect on contractile responses induced by porcine pancreatic PLA₂. LY311727 nearly abolished the hnpS-PLA₂ responses at 10 μM , while it failed to suppress porcine pancreatic PLA₂ concentration response curves at the same concentration (Fig. 5b). This observation, using an isolated tissue preparation as the substrate for these enzymes, is also in agreement with LY311727 being only a weak inhibitor of porcine pancreatic PLA₂ in the chromogenic isolated enzyme assay (0.029 mole fraction). Furthermore, contractions induced by arachidonic acid were not inhibited by LY311727 (Table 1), indicating no CO activity. Thus these data clearly illustrate the selectivity of LY311727 as an inhibitor of hnpS-PLA₂.

A drug design success?

Application of structure based drug design to the hnpS-PLA₂ target has provided LY311727, the first potent and selective inhibitor of this secretory enzyme. This compound has shown fifty percent inhibition of substrate hydrolysis by the human, Group II (ref. 27) enzyme at a concentration that is 20,000 times less than the phospholipid substrate concentration. Furthermore, the inhibitor is 1,500-fold selective when assayed against the structurally similar porcine pancreatic (Group I) enzyme. This level of selectivity was also demonstrated for the first time on guinea pig lung tissue, a natural membrane substrate. Collectively, these data make it clear that LY311727 has been exquisitely tailored to fit the active site of hnpS-PLA₂ through tight and specific binding interactions. These optimization efforts also led to the

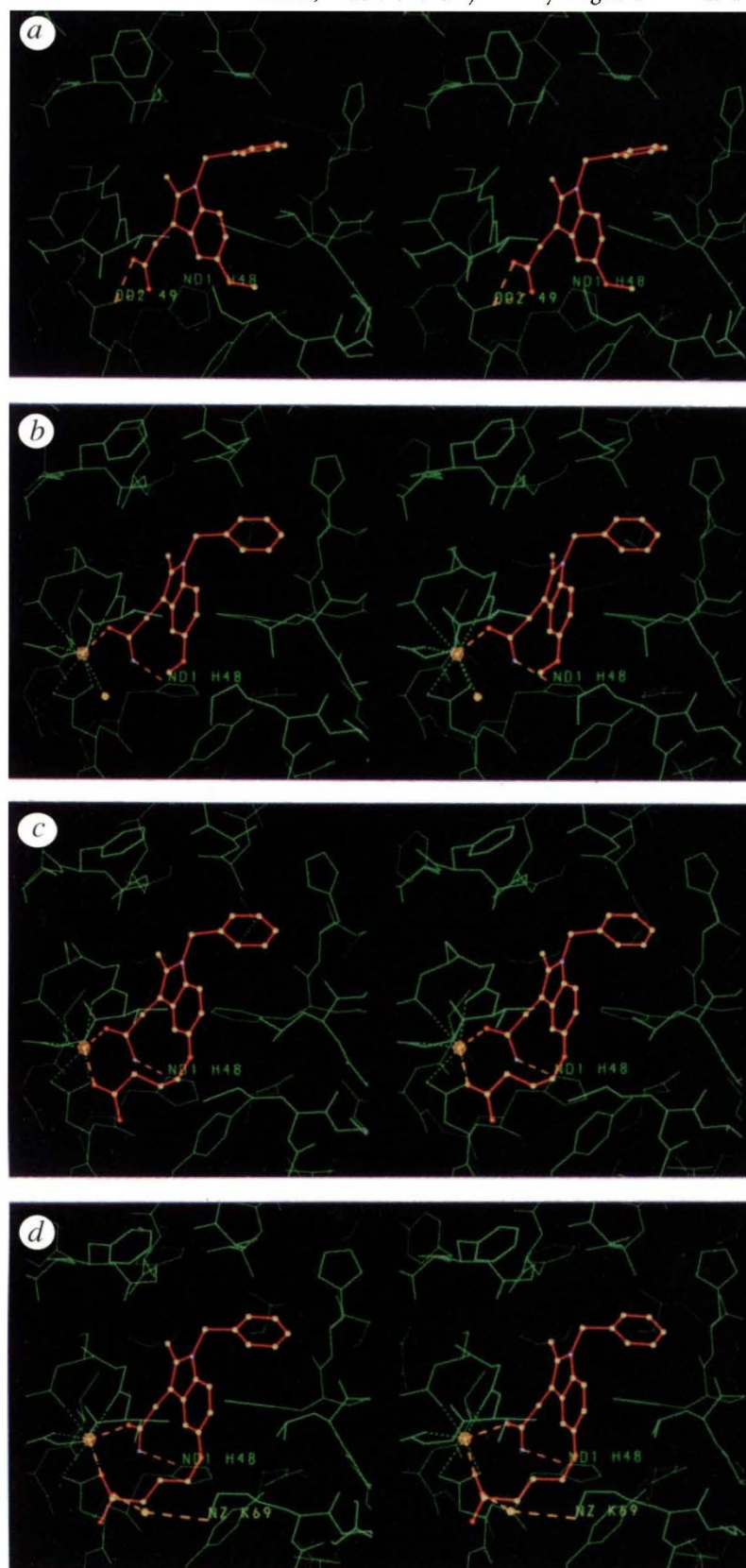


Fig. 4 The binding of indole inhibitors (red) to hnpS-PLA₂ (green) in the active site. Interactions between calcium (large yellow sphere) and enzyme or water ligands (yellow sphere) are shown with dotted lines. Inhibitor interactions are shown with dashed lines. *a*, Indole 1 does not contain an active site calcium and hydrogen bonds directly to O δ 2 of Asp 49. No hydrogen bond is made to His 48. *b*, Indole 3 contributes one ligand to active site calcium through amide oxygen and hydrogen bonds to N δ 1 of His 48. *c*, Indole 6 contributes two ligands to calcium, one through its amide oxygen and one through its carboxylate. The hydrogen bond to His 48 is formed. *d*, Indole 8 contributes two oxygen ligands to calcium, one through its amide and one through its phosphonate. One phosphonate oxygen also hydrogen bonds to Lys 69 through an intervening water molecule. The hydrogen bond to His 48 is formed.

complete elimination of nonspecific effects, including CO activity, making this a truly selective hnpS-PLA₂ inhibitor.

The underlying ideas behind development of this hnpS-PLA₂ inhibitor have been empirically based. A lead compound from large scale screening of library compounds was obtained and its mode of binding to hnpS-PLA₂ determined crystallographically. This was important because large movements of side chains that were necessary to accommodate these inhibitors could not have been reliably predicted from the native structure. Although a similar movement of His 6 seen in the crystal structure of TSA with hnpS-PLA₂ demonstrates the possibility of this change in the protein, it is not necessarily a feature of all inhibitor binding. The displacement of the flap residue Lys 69 in response to indole 1 binding, but not seen with indoles 3, 6 or 8, was not observed in either native or substrate analogue structures. The use of both empirical screening methods to identify the lead compound and crystallography to reveal structural details of binding were essential to success.

An important part of these molecules' potency comes from their structural core. The initial acetamide, indole 3, has potency comparable to or better than that of TSA and ASA, even though it has less lipophilic contact surface and fewer polar and charged interactions with enzyme. A likely explanation for this is the constraints imposed by the indole ring and benzyl group which allow these inhibitors only a small number of conformations, one of which is fortuitously in the right shape for interacting with the PLA₂ cavity.

It is useful to broadly consider the factors contributing to the 737-fold improvement in potency achieved in

this series of hnpS-PLA₂ inhibitors. Most of this increase in binding has come from the addition or modification of polar or charged groups to enhance interactions with complementary groups of the enzyme. The conversion of the 3-position acetate to an acetamide provides a hydrogen bond to His 48 reminiscent of that documented for ASA, and also permits direct interaction with the active site calcium ion rather than displacement of it. Addition of an extension at the 5-position which is terminated with an acidic function mimics the phosphate groups of both ASA and TSA by coordinating to the catalytic calcium. Optimally fitting a small hydrophobic cleft at the 2-position also results in a corresponding increase in potency. While each change by itself has led to an incremental (3- to 20-fold) improvement, the summation of all of these changes impart a dramatic increase in potency to the molecule. This iterative process of structure analysis, synthesis and kinetic analysis used for the development of LY311727 affirms the great power of these techniques in drug discovery activities.

Methods

Crystallography. The protein was cloned, expressed and purified as described¹⁷. The crystals of the complexes were prepared by co-crystallization with the various inhibitors. The crystals were grown by vapour diffusion in about two weeks from a solution containing 10.0 mg ml⁻¹ of protein in 50 mM buffer (MES or MOPS), pH 6.6–7.5, 80–92 % saturated in sodium chloride, 1 % pyridine. An inhibitor concentration of 1.5 molar equivalent was used. The X-ray diffraction data collection and processing were done by using the RAXIS II system with imaging plate detector and rotating anode X-ray source (CuK α radiation, $\lambda = 1.542 \text{ \AA}$)¹¹. The structure of indole 1 was solved by the molecular replacement method using the X-PLOR program package²⁹. The starting model was the enzyme native structure solved and described previously¹⁷. The

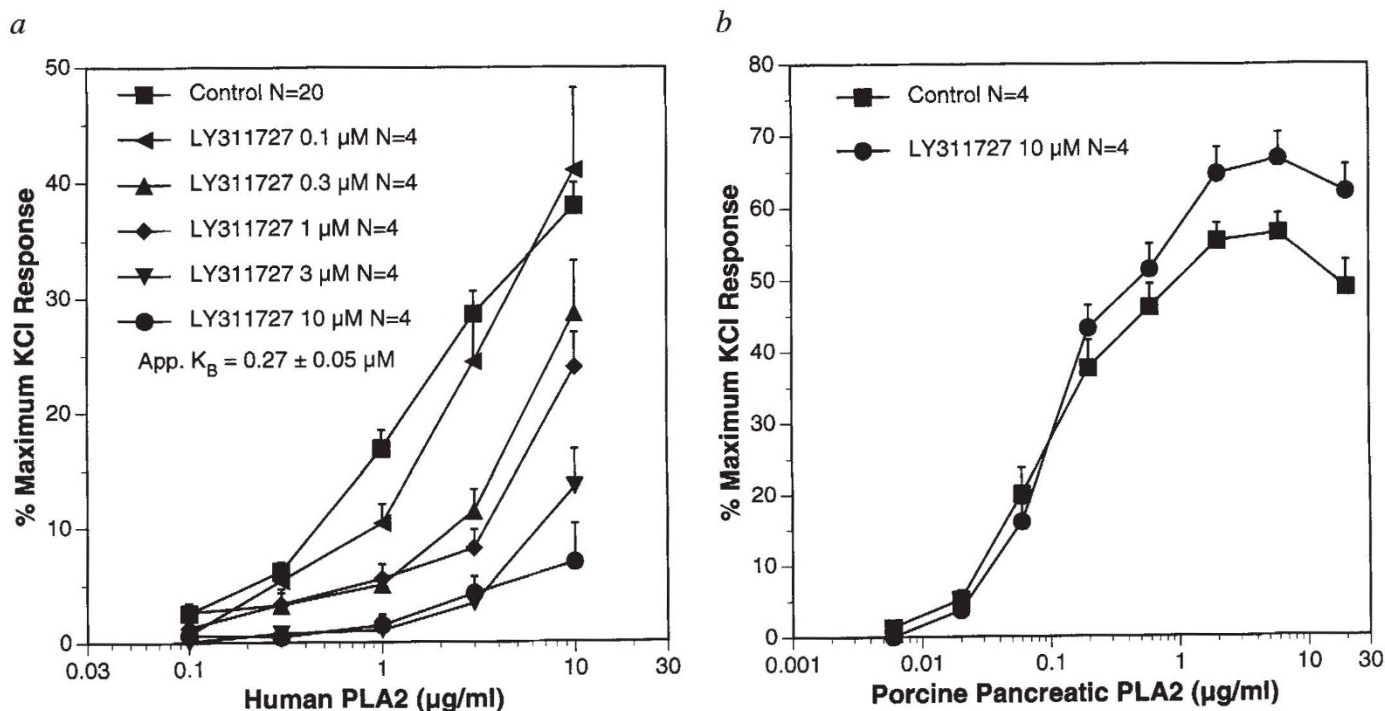


Fig. 5 The effect of LY311727 on *a*, human sPLA₂ and *b*, porcine pancreatic PLA₂ concentration-response curves for guinea pig lung pleural strips.

structure was refined alternatively using X-PLOR and PROLSQ³⁰. The quality of the model was analyzed and improved at intervals using the molecular graphics program FRODO³¹. The structures of indoles **3**, **6** and **8** were solved using the structure of indole **1** as the starting model. Coordinates will be deposited in the Brookhaven Protein Data Bank.

Assays. Indoles (**1**) were evaluated in a modified chromogenic assay²⁴ containing final concentrations of 0.96 mM racemic 1,2 bis(thioheptanoyl)-1,2-dideoxyphosphatidylcholine (PC), 0.27 mM Triton X-100 (T) and 0.12 mM 5,5'-dithiobis(2-nitrobenzoic acid). Concentration/response curves were generated with 16 nM recombinant hnp-PLA₂ for 30 min. at 40 °C in a microtiter plate

format. Mole fractions ($([I]/([I]+[PC]+[T]))$) for 50% inhibition, $X_i(50)$, were determined in triplicate; standard deviations were +/- 10–50%. Inhibitors were tested against guinea pig pleural strips challenged with either hnp-PLA₂ or arachidonic acid (AA) as described previously²⁵. For the concentration-response curves on guinea pig pleural strips, LY311727 was incubated with the tissues for 30 min. prior to starting the PLA₂ concentration-response curves. Data were pooled from individual experiments and are expressed as percentage of maximal KCl (40 mM) responses (means ± sem from (N) number of paired tissues). Tissues were prepared as previously described²⁵.

Received 15 March; accepted 25 April 1995.

Acknowledgements

We thank C. Teater for purification of hnp-PLA₂, D. Hunden for the preparation of chromogenic substrate and D. Berry and E. Mc Kinney for assay support.

- Green, J.-L. *et al.* Circulating phospholipase A₂ activity associated with sepsis and septic shock is indistinguishable from that associated with rheumatoid arthritis. *Inflammation* **15**, 355–367 (1991).
- Kramer, R. M. *et al.* Structure & properties of a human non-pancreatic phospholipase A₂. *J. Biol. Chem.* **264**, 5768–5775 (1989).
- Dennis, E.A., Rhee, S.G., Billah, M.M. & Hannun, Y.A. Role of phospholipases in generating lipid second messengers in signal transduction. *FASEB J.* **5**, 2068–2077 (1991).
- Pruzanski, W., Vadas, P. & Browing, J. Secretory non-pancreatic group II phospholipase A₂: role in physiologic and inflammatory processes. *J. Lipid Med.* **8**, 161–167 (1993).
- Santos, A.A. *et al.* Are events after endotoxemia related to circulating phospholipase A₂? *Ann. Surg.* **219**, 183–192 (1994).
- Vadas, P. & Pruzanski, W. Induction of group II phospholipase A₂ expression and pathogenesis of the sepsis syndrome. *Circ. Shock* **39**, 160–167 (1993).
- Baldwin, J. J. *et al.* Thienopyran-2-sulfonamides: novel topically active carbonic anhydrase inhibitors for the treatment of glaucoma. *J. med. Chem.* **32**, 2510–2513 (1989).
- Shoichet B.K., Stroud R.M., Santi, D.V., Kuntz, I.D. & Perry, K.M. Structure-based discovery of inhibitors of thymidylate synthase. *Science* **259**, 1445–1450 (1993).
- Erickson, J. *et al.* Design, activity, and 2.8 Å crystal structure of a C₂ symmetric inhibitor complexed to HIV-1 protease. *Science* **249**, 527–533 (1990).
- Lam, P.Y.S. *et al.* Rational design of potent, bioavailable, nonpeptide cyclic ureas as HIV protease inhibitors. *Science* **263**, 380–384 (1994).
- Ealick, S.E. *et al.* Application of crystallographic and modelling methods in the design of purine nucleoside phosphorylase inhibitors. *Proc. Natn. Acad. Sci. U.S.A.* **88**, 11540–11544 (1991).
- von Itzstein, M. *et al.* Rational design of potent sialidase-based inhibitors of influenza virus replication. *Nature* **363**, 418–423 (1993).
- Warner, P., Green, R.C., Gomes, B. & Strimpler, A.M. Non-peptide inhibitors of human leukocyte elastase. 1. The design and synthesis of pyridone-containing inhibitors. *J. med. Chem.* **37**, 3090–3099 (1994).
- Beaton, H.G. *et al.* Discovery of new non-phospholipid inhibitors of the secretory phospholipases A₂. *J. med. Chem.* **37**, 557–559 (1994).
- Jain, M.K. *et al.* Fatty acid amides: scouting mode-based discovery of tight-binding competitive inhibitors of secreted phospholipases A₂. *J. med. Chem.* **35**, 3584–3586 (1992).
- Pisabarro, M.T. *et al.* Rational modification of human synovial fluid phospholipase A₂ inhibitors. *J. med. Chem.* **37**, 337–341 (1994).
- Wery, J.-P. *et al.* Structure of recombinant human rheumatoid

arthritic synovial fluid phospholipase A₂ at 2.2 Å resolution. *Nature* **352**, 79–82 (1991).

- Scott, D.L. *et al.* Structures of free and inhibited human secretory phospholipase A₂ from inflammatory exudate. *Science* **254**, 1007–1010 (1991).
- White, S.P., Scott, D.L., Otwinowski, Z., Gelb, M.H. & Sigler, P.B. Crystal structure of cobra-venom phospholipase A₂ in a complex with a transition-state analogue. *Science* **250**, 1560–1563 (1990).
- Scott, D.L., Otwinowski, Z., Gelb, M.H. & Sigler P.B. Crystal structure of bee venom phospholipase A₂ in a complex with a transition-state analogue. *Science* **250**, 1563–1566 (1990).
- Thunnissen, M.M.G.M. *et al.* X-ray structure of phospholipase A₂ complexed with a substrate-derived inhibitor. *Nature* **347**, 689–691 (1990).
- Kaplan, L., Weiss, J. & Elsbäck, P. Low concentrations of indomethacin inhibit phospholipase A₂ of rabbit polymorphonuclear leukocytes. *Proc. natn. Acad. Sci. U.S.A.* **75**, 2955–2958 (1978).
- Lobo, I.B. & Hoult, J.R.S. Groups I, II and III extracellular phospholipases A₂: Selective inhibition of group II enzymes by indomethacin but not other NSAIDs. *Agents Actions* **41**, 111–113 (1994).
- Reynolds, L.J., Hughes, L.L. & Dennis, E.A. Analysis of human synovial fluid phospholipase A₂ on short chain phosphatidylcholine-mixed micelles: development of a spectrophotometric assay suitable for a microtiterplate reader. *Analyt. Biochem.* **204**, 190–197 (1992).
- Snyder, D.W., Sommers, C.D., Bobbitt, J.L. & Mihelich, E.D. Characterization of the contractile effects of human recombinant non-pancreatic secretory phospholipase A₂ and other PLA₂s on guinea pig lung pleural strips. *J. Pharmac. exp. Ther.* **266**, 1147–1155 (1993).
- Yu, L. & Dennis, E.A. Critical role of a hydrogen bond in the interaction of phospholipase A₂ with transition-state and substrate analogues. *Proc. natn. Acad. Sci. U.S.A.* **88**, 9325–9329 (1991).
- Dennis, E.A. Diversity of group types, regulation, and function of phospholipase A₂. *J. Biol. Chem.* **269**, 13057–13060 (1994).
- Shibata, A. Diffraction data collection with R-Axis II, an X-ray detecting system using imaging plate. *Rigaku J.* **7**, 28–32 (1990).
- Brunger, A. *X-PLOR version 3.1 A system for crystallography and NMR.* (Yale Univ. Press, New Haven and London; 1992).
- Hendrickson, W.A. & Konnert, J.H. Stereochemically restrained least-squares refinement. in *Biomolecular Structure, Function, Conformation and Evolution* (ed. Srinivasan, R.) 43–57 (Pergamon, Oxford; 1981).
- Jones, T.A. A graphics model building and refinement system for macromolecules. *J. appl. Crystallogr.* **11**, 268–272 (1978).